The EMBO Journal Vol.17 No.11 pp.3016–3028, 1998

$P2X_1$ and $P2X_3$ receptors form stable trimers: a novel structural motif of ligand-gated ion channels

Annette Nicke, Hans G.Bäumert[1], Jürgen Rettinger, Annette Eichele, Günter Lambrecht, Ernst Mutschler and Günther Schmalzing[2]

Biocenter of the Johann Wolfgang Goethe–University of Frankfurt, Department of Pharmacology and [1]Department of Biochemistry, Marie-Curie-Strasse 9, D-60439 Frankfurt, Germany

[2]Corresponding author
e-mail: schmalzing@em.uni-frankfurt.de

P2X receptors are cation channels gated by extracellular ATP. The seven known P2X isoforms possess no sequence homology with other proteins. Here we studied the quaternary structure of P2X receptors by chemical cross-linking and blue native PAGE. $P2X_1$ and $P2X_3$ were N-terminally tagged with six histidine residues to allow for non-denaturing receptor isolation from cRNA-injected, [^{35}S]methionine-labeled oocytes. The His-tag did not change the electrophysiological properties of the $P2X_1$ receptor. His-$P2X_1$ was found to carry four N-glycans per polypeptide chain, only one of which acquired Endo H resistance en route to the plasma membrane. 3,3′-Dithio*bis*(sulfosuccinimidylpropionate) (DTSSP) and two of three bifunctional analogues of the P2X receptor antagonist pyridoxalphosphate-6-azophenyl-2′,4′-disulfonic acid (PPADS) cross-linked digitonin-solubilized His-$P2X_1$ and His-$P2X_3$ quantitatively to homo-trimers. Likewise, when analyzed by blue native PAGE, P2X receptors purified in digitonin or dodecyl-β-D-maltoside migrated entirely as non-covalently linked homo-trimers, whereas the $\alpha_2\beta\gamma\delta$ nicotinic acetylcholine receptor (used as a positive control) migrated as the expected pentamer. P2X monomers remained undetected soon after synthesis, indicating that trimerization occurred in the endoplasmic reticulum. The plasma membrane form of His-$P2X_1$ was also identified as a homo-trimer. If *n*-octylglucoside was used for P2X receptor solubilization, homo-hexamers were observed, suggesting that trimers can aggregate to form larger complexes. We conclude that trimers represent an essential element of P2X receptor structure.

Keywords: blue native PAGE/cross-linking/P2X receptor/quaternary structure/*Xenopus laevis* oocytes

Introduction

Receptors activated by extracellular ATP are designated P2 receptors and are represented by two major protein families: (i) a P2Y metabotropic receptor family of G-protein-coupled receptors; and (ii) a P2X ionotropic receptor family (Abbracchio and Burnstock, 1994). The P2X receptors are cation-selective, ligand-gated ion channels that open in the millisecond range in response to the binding of extracellular ATP (for reviews see Buell *et al*., 1996a; Burnstock, 1996). They play a role in fast synaptic transmission between neurons, from neurons to smooth muscle and in ATP-mediated lysis of antigen-presenting cells. To date seven P2X isoforms designated $P2X_{1–7}$ have been cloned from various tissues including smooth muscle and neuronal cells (for references see Buell *et al.*, 1996a). The human isoforms $P2X_1$, $P2X_4$ and $P2X_7$ have also been cloned (Valera *et al.*, 1995; Garcia-Guzman *et al.*, 1997; Rassendren *et al.*, 1997b). The deduced rat proteins, 379–595 amino acids long, show sequence identities (35–48%) between themselves with similar distributions of hydrophilic and hydrophobic domains. Heterologous expression of P2X isoforms results in the formation of functional P2X receptors with electrophysiological and pharmacological profiles similar to that of P2X receptors in native tissues.

Channel proteins known so far are transmembrane symmetric or pseudosymmetric oligomers arranged such that polar residues line a central ion-conducting hydrophilic pore. The structure of nicotinic acetylcholine receptor (nAChR), currently the best characterized ligand-gated channel, has been determined at 9 Å resolution (Unwin, 1995; Hucho *et al.*, 1996). It is a pentamer of homologous or identical subunits, surrounding a central water-filled pore that conducts cations when its opening is triggered by ligand binding. Since glycine, $GABA_A$ and 5-HT_3 receptor subunits share extensive sequence homology with nAChR subunits, they are all thought to have evolved from a common ancestor and to constitute a gene superfamily (Betz, 1990; Ortells and Lunt, 1995). All superfamily members fold into four transmembrane domains (M1–M4) with the N and C termini both located extracellularly (for review see Dani and Mayer, 1995). It is generally accepted that M2 is α-helical and the main contributor to the channel lining (Unwin, 1995; Hucho *et al.*, 1996). A pentameric structure has also been demonstrated for glycine (Langosch *et al.*, 1988), $GABA_A$ (Nayeem *et al.*, 1994) and 5-HT_3 receptors (Boess *et al.*, 1995), indicating that the members of the ligand-gated ion channel superfamily share a conserved quaternary structure.

Ionotropic glutamate receptors encompassing the AMPA, kainate and NMDA types constitute a second class of ligand-gated ion channels distinct from the receptor superfamily mentioned above (Hollmann and Heinemann, 1994). Like the nAChR superfamily members, glutamate receptor subunits possess four hydrophobic domains. From these only M1, M3 and M4 cross the membrane, whereas M2 forms a re-entrant membrane loop with both ends facing the cytoplasm (for references see Dani and Mayer, 1995). The M2 re-entrant loop has been shown to play an

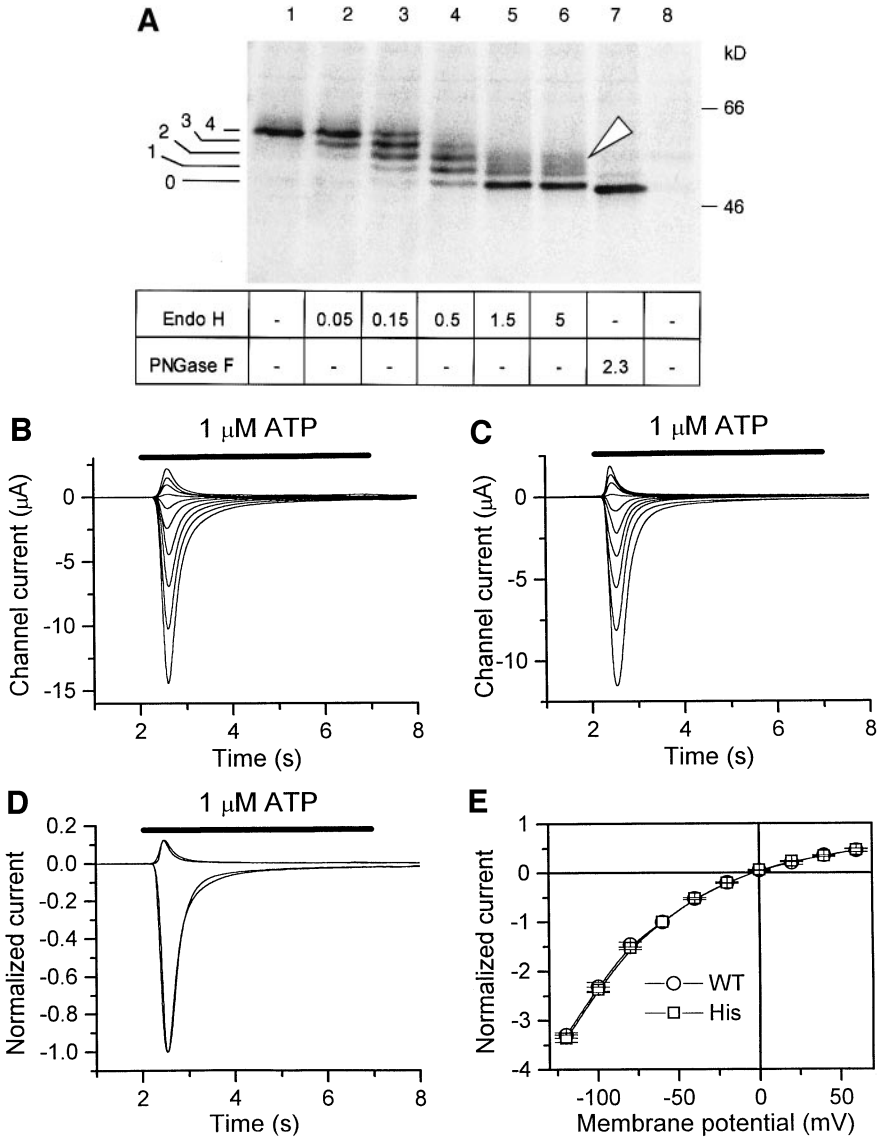

Fig. 1. Biochemical and functional characterization of rat His-$P2X_1$. Oocytes were injected with 25 ng cRNA for wt-$P2X_1$ or His-$P2X_1$. (**A**) After a 6 h [^{35}S]methionine pulse and a 12 h chase, oocytes were extracted with 1% *n*-octylglucoside. His-$P2X_1$ was purified by Ni^{2+}-agarose chromatography, eluted with non-denaturing elution buffer, and then supplemented with SDS sample buffer, 20 mM DTT (final concentration) and Endo H or PNGase F (in IUB milliunits per 10 μl sample) as indicated. After 1 h at 37°C, samples were analyzed by SDS–PAGE (10% acrylamide) followed by autoradiography. Lane 8, non-injected controls; lanes 1–7, His-$P2X_1$ cRNA-injected oocytes. Arrow indicates position of complex-glycosylated His-$P2X_1$; positions of deglycosylation intermediates are indicated by numbers 1–3 on left margin, 0 and 4 correspond to the protein core and the core-glycosylated form, respectively, of His-$P2X_1$. (B, C) After 3 days at 19°C, current responses of wt-$P2X_1$ (**B**) and His-$P2X_1$ (**C**) were elicited at holding potentials from –120 to +60 mV by application of 1 μM ATP for 5 s in 1 min intervals. Representative original current responses are shown. No corrections except background subtraction were applied to the data. (**D**) Responses of wt-$P2X_1$ and His-$P2X_1$ shown in (B) and (C), respectively, at –120 mM and +60 mV were normalized to the peak response at –120 mV to demonstrate the virtual identical time course of desensitization of both receptor types. (**E**) Current–voltage dependencies of wt-$P2X_1$ (○) and His-$P2X_1$ (□) were derived as described in (B) and (C). Peak currents at the different potentials were normalized to the peak response at –60 mV and averaged. Mean currents (± standard error, $n = 6$) elicited in 1 min intervals at –60 mV were –2.9 ± 0.3 μA and –3.2 ± 0.4 μA for wt-$P2X_1$ and His-$P2X_1$, respectively.

important role in channel lining (Kuner *et al.*, 1996). For the ionotropic glutamate receptor family, a pentameric subunit organization was reported (Ferrer-Montiel and Montal, 1996), whereas more recent evidence suggests a tetrameric structure (Laube *et al.*, 1998; Mano and Teichberg, 1998).

P2X subunit isoforms do not exhibit significant sequence homology with any of the other ligand-gated ion channels and are therefore considered to represent a third major class of ligand-gated ion channels (North, 1996b). The absence of a cleaved N-terminal signal sequence places the N terminus on the cytoplasmic side of the membrane. Protein topology predicts only two membrane-spanning segments, M1 and M2, connected by an N-glycosylated ectodomain of ~270 amino acids (North, 1996b). The usage of naturally occurring N-glycosylation sites (see present study) and the identification of residues that contribute to the channel pore (Rassendren *et al.*, 1997a) suggest that the predicted membrane topology is essentially correct. By probing the accessibility of engineered cysteine residues to sulfhydryl-specific reagents, the M2 domain has been demonstrated to be involved in pore formation of

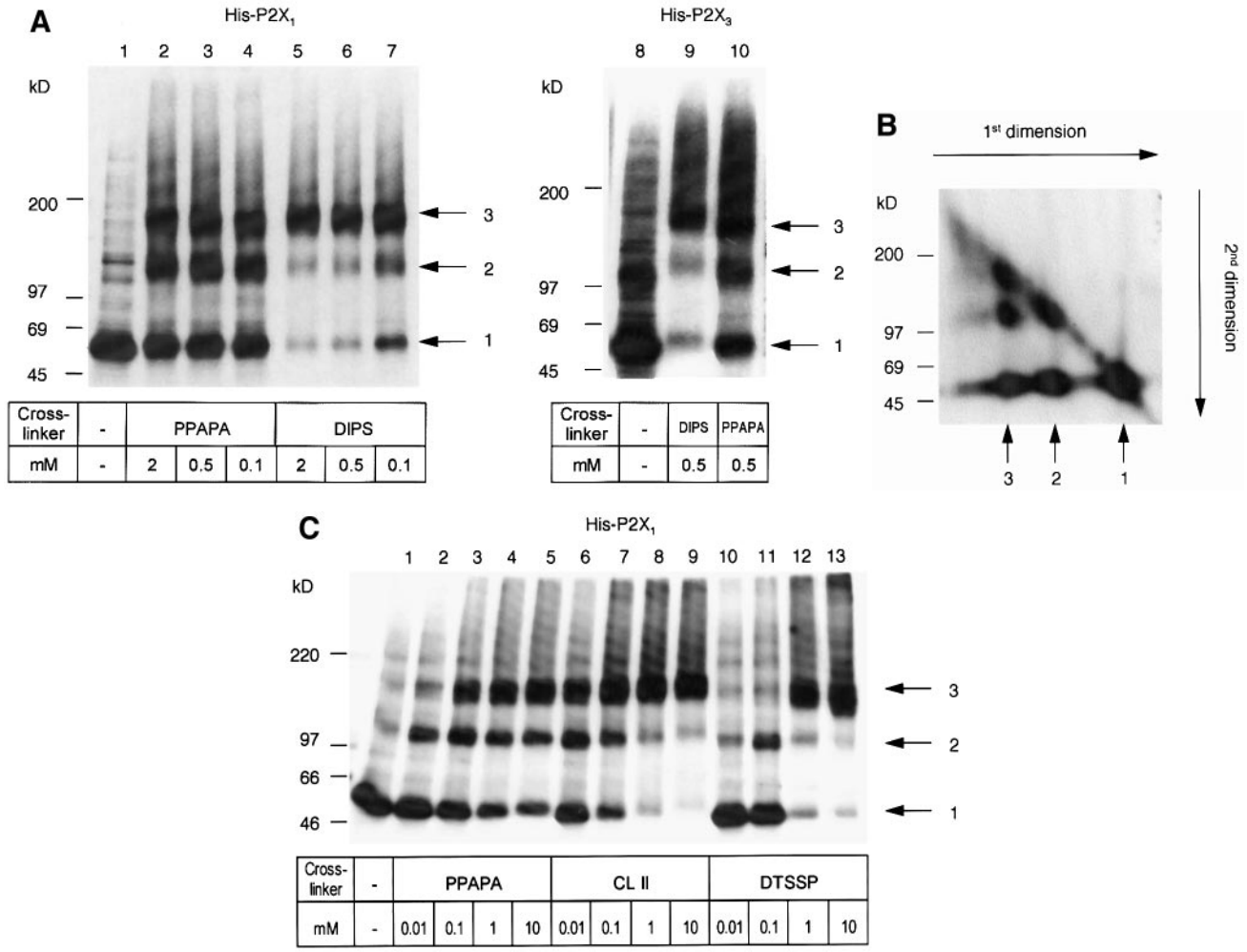

Fig. 2. Cross-linking of digitonin-solubilized, purified His-P2X$_1$ and His-P2X$_3$. Oocytes injected with the indicated cRNAs were labeled overnight with [^{35}S]methionine and chased for 5–10 h. Digitonin extracts (0.5%) were then prepared and P2X receptors were purified by Ni^{2+}-agarose chromatography. Numbered arrows indicate positions of P2X monomers, dimers and trimers. (**A**) P2X receptors were incubated with the indicated cross-linkers and $NaBH_4$ while still bound to the beads. After elution with non-denaturing elution buffer, samples were supplemented with SDS sample buffer and 20 mM DTT and resolved by SDS–PAGE (4–10% acrylamide gradient gel) followed by autoradiography. (**B**) An aliquot of the His-P2X$_1$ sample cross-linked at 2 mM PPAPA was resolved in the first dimension by SDS–PAGE (4–10% acrylamide gradient gel). The gel lane was then excised, treated for 30 min with 30 mM sodium dithionite in SDS stacking gel buffer at ambient temperature, and re-analyzed by SDS–PAGE (4–10% acrylamide gradient gel) in the second dimension. (**C**) P2X receptors were first eluted with non-denaturing elution buffer, then incubated with PPAPA, DTSSP or CL II as indicated, and reduced with $NaBH_4$. Samples cross-linked with DTSSP were not treated with $NaBH_4$. All the samples were supplemented with SDS sample buffer and resolved by non-reducing SDS–PAGE (4–10% acrylamide gradient gel).

the P2X$_2$ isoform. Interestingly, however, the accessibility patterns are in line with a β-sheeted secondary structure for at least part of the pore rather than with an α-helical structure (Rassendren *et al.*, 1997a). P2X receptors share their membrane topology with a variety of channel proteins including the epithelial Na^+ channel/degenerin gene superfamily (North, 1996a). One branch of this superfamily, the FMRFamide peptide-gated Na^+ channel of *Helix aspersa* (Linguelia *et al.*, 1995), shares with P2X the property of being ligand-activated and can be considered to constitute a fourth class of ligand-gated ion channels.

Given that the membrane topology of P2X receptors and presumably also the pore region is fundamentally different from that of the other two major classes of ligand-gated ion channels, the oligomeric organization of P2X receptors is of great interest. To address this issue, we adapted the blue native PAGE system (Schägger and von Jagow, 1991; Schägger *et al.*, 1994) for the analysis of P2X receptors which were heterologously expressed in *Xenopus laevis* oocytes. Oocytes have been used successfully for the determination of the quaternary structure of nAChR (Anand *et al.*, 1991). In addition, we examined a series of bifunctional derivatives of the P2 receptor antagonist pyridoxalphosphate-6-azophenyl-2′,4′-disulfonic acid (PPADS; Lambrecht, 1996) which turned out to be highly effective cross-linkers of P2X$_1$ and P2X$_3$ receptors. Our results indicate that trimeric complexes of identical subunits constitute an essential structural element of P2X receptor channels.

Results

His-tagged P2X$_1$ and P2X$_3$ receptors are functional in Xenopus oocytes

To isolate P2X receptors after synthesis in *Xenopus* oocytes, we have tagged the proteins at their N-terminal end with a hexahistidyl sequence. SDS–PAGE analysis revealed that His-P2X$_1$ (Figure 1A, lane 1) was synthesized

as a 57 kDa protein. Treatment with peptide:*N*-glycosidase F (PNGase F) to release N-glycans completely from both high mannose and complex types of glycoproteins reduced the molecular mass to 47 kDa (Figure 1A, lane 7), close to the mass of the His-tagged protein core computed from the cDNA sequence. Deglycosylation with increasing concentrations of endoglycosidase H (Endo H) generated a total of five bands (Figure 1A, lanes 2–4) that differ in mass by 2–3 kDa, i.e. the mass of an N-linked oligosaccharide side chain. Since the 47 kDa band represents the core protein, the other bands correspond to the core-glycosylated $P2X_1$ protein and three deglycosylation intermediates. We conclude from these data that $P2X_1$ carries four N-glycans when synthesized in oocytes, i.e. that four out of the five potential N-glycosylation sites of $P2X_1$ (Valera *et al.*, 1994) are used. Within 20 h from the beginning of [^{35}S]methionine labeling, 43% of His-$P2X_1$ acquired Endo H-resistant, complex-type carbohydrates as assessed by phosphor image analysis (Figure 1A, lanes 5–6). Since Endo H removes N-linked chains only as long as they have not been complex-glycosylated by the Golgi enzymes, this indicates that a significant fraction of His-$P2X_1$ is able to leave the endoplasmic reticulum (ER) and to reach the Golgi apparatus and later compartments such as the plasma membrane.

To examine whether the N-terminal hexahistidyl sequence affects the function of P2X receptors, two-electrode voltage clamp measurements were carried out on cRNA-injected oocytes. Figure 1B and C displays original current traces of wild-type and His-$P2X_1$ receptors activated by 1 μM ATP in 1 min intervals and recorded at different membrane potentials ranging from –120 to +60 mV. Please note that the currents recorded after repetitive application of ATP were ~10-fold smaller than those elicited by a first ATP addition to oocytes, i.e. before desensitization of P2X receptors. Normalization of the current traces from Figure 1B and C at –120 and +60 mM to the response at –120 mV revealed that the time courses of receptor desensitization of wild-type $P2X_1$ and His-$P2X_1$ were virtually identical (Figure 1D). Also the current–voltage dependencies of wild-type $P2X_1$ and His-$P2X_1$ were virtually identical (Figure 1E). We conclude from these results that capping the N terminus of $P2X_1$ by a hexahistidyl sequence does not notably affect the functional properties of the $P2X_1$ receptor. Likewise, the hexahistidyl tag did not interfere with the function of the His-$P2X_3$ receptor channel (data not shown).

Cross-linking of purified $P2X_1$ or $P2X_3$ receptors generates dimers and trimers

When digitonin-solubilized His-$P2X_1$ was denatured with SDS and resolved by non-reducing SDS–PAGE, five (Figure 2C, lane 1) to six protein bands were observed in addition to the prominent band of His-$P2X_1$ monomers. The additional protein bands corresponded in size to His-$P2X_1$ multimers and disappeared when the gel was run under reducing conditions (Figure 2A, lane 1). Inclusion of up to 100 mM iodoacetamide during all purification steps to hinder cross-linking of His-$P2X_1$ monomers by artificial disulfide bonds did not prevent the occurrence of the SDS-resistant His-$P2X_1$ multimers. We interpreted the SDS–PAGE pattern as an indication of the oligomeric

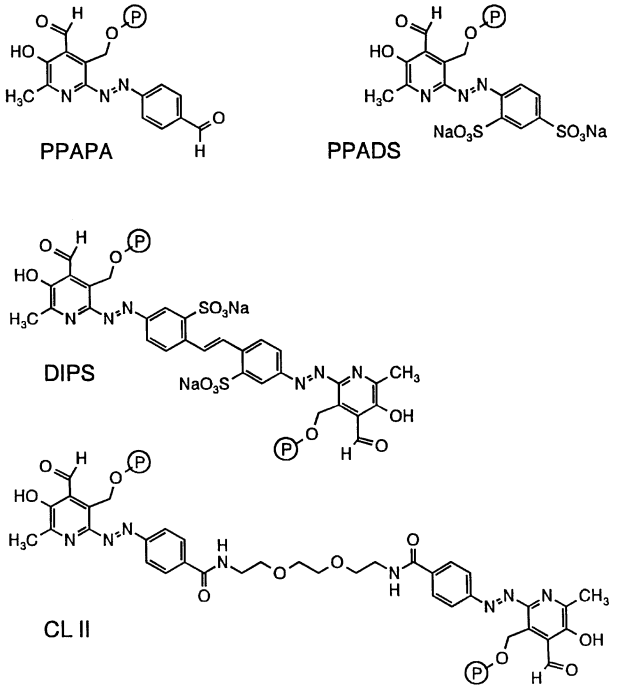

Fig. 3. Structures of PPADS and bifunctional PPADS analogues.

state of the protein (Doms and Helenius, 1986) and applied cross-linkers to increase the yield of His-$P2X_1$ multimers.

In initial experiments, we used dithio*bis*(succinimidyl-propionate) (DSP) and 3,3′-dithio*bis*(sulfosuccinimidyl-propionate) (DTSSP) in addition to the P2X receptor antagonist 4,4′-diisothiocyanatostilbene-2,2′-disulfonic acid (DIDS; Bültmann *et al.*, 1996) to cross-link His-$P2X_1$ subunits in intact oocytes and oocytes permeabilized at 100 μM (0.012%) digitonin (Schmalzing *et al.*, 1989). All three compounds were able to link $P2X_1$ subunits to dimers and trimers, but even at millimolar concentrations of either compound most of the $P2X_1$ receptor protein was found to be in the monomeric form when analyzed by SDS–PAGE (results not shown).

Next, we cross-linked His-$P2X_1$ receptors subsequent to purification while still bound to the Ni^{2+}-agarose beads. DIDS cross-linked purified $P2X_1$ subunits to dimers and trimers, but was not used further because it decreased the yield of $P2X_1$ protein, apparently by interfering with the binding to the Ni^{2+}-nitrilotriacetate (NTA) agarose (data not shown). However, the ability of DIDS to cross-link $P2X_1$ prompted us to investigate bifunctional analogues of the P2X receptor antagonist PPADS (Lambrecht, 1996). Structures are shown in Figure 3. PPADS carries an aldehyde group that is capable of forming a Schiff base with a primary amino group as shown for the parent compound, pyridoxal 5-phosphate (Cake *et al.*, 1978). PPAPA lacks the sulfonic acid groups of PPADS, but possesses a second aldehyde function, whereas DIPS and CL II can be considered to be composed of two PPADS-like molecules linked by spacers of distinct length and conformational flexibilities. The spacer of DIPS consists of a DIDS molecule lacking its isothiocyano groups. When added to digitonin-solubilized, purified His-$P2X_1$, all the three PPADS analogues cross-linked $P2X_1$ subunits to dimers and trimers at concentrations as low as 10 μM (Figure 2A and C). It should be noted that we reduced

the chemically labile C=N bond of Schiff bases with borohydride to a stable amine bond. Virtually identical results were obtained irrespective of whether cross-linking was performed with digitonin-solubilized $P2X_1$ while still bound to Ni^{2+}-NTA agarose (Figure 2A) or subsequent to non-denaturing elution from Ni^{2+}-agarose (Figure 2C). Also cross-linking of the P2X isoform $P2X_3$ yielded dimers and trimers (Figure 2A, lanes 9–10). The relative amounts of dimers and trimers produced depended on the distance between the two reactive groups of the cross-linkers. The relatively rigid PPAPA molecule, having a distance of ~11 Å between its two aldehyde functions, produced similar amounts of $P2X_1$ dimers and trimers. Increasing the length and flexibility of the spacer led to a preferential formation of trimers (Figure 2A and C). At ⩾1 mM, DIPS (Figure 2A) and CL II (Figure 2C) were able to cross-link $P2X_1$ subunits almost quantitatively to trimers. CL II possesses an extremely long and flexible spacer of ~34 Å between the two aldehyde functions. The widely used cross-linker DTSSP with two reactive groups ~12 Å apart from each other was also capable of cross-linking $P2X_1$ subunits almost quantitatively to trimers. However, in the 10–100 μM range, DTSSP was markedly less efficient than CL II (Figure 2C). Diepoxybutane, a cross-linker with a very short molecular span, produced His-$P2X_1$ dimers in some of the experiments, but failed to induce significant cross-linking in several others (results not shown).

The azo bond of PPAPA, DIPS and CL II can be cleaved with dithionite. To examine whether the protein adducts were entirely composed of cross-linked His-$P2X_1$ monomers, samples were first separated by SDS–PAGE in the first dimension, then treated with dithionite and finally re-analyzed in the second dimension by SDS–PAGE (Lutter *et al.*, 1974). Dithionite treatment generated dimers and monomers, but no intermediate cleavage products, indicating that the multimers consisted solely of $P2X_1$ subunits (Figure 2B).

The long-lasting blockade of certain P2X receptor subtypes by PPADS has been attributed to its aldehyde group that can react with a lysine residue to form a Schiff base. Based on a previous report (Buell *et al.*, 1996b) demonstrating that substitution of lysine for Glu249 of PPADS-insensitive rat $P2X_4$ receptors confers high and irreversible PPADS sensitivity, we mutated Lys249 at the equivalent position of $P2X_1$ to Ser. Mutant His-$P2X_1$-K249S could be cross-linked with DIPS as efficiently as His-$P2X_1$ itself (results not shown). This indicates that lysine residues other than Lys249 must be involved in the cross-linking reaction.

$P2X_1$ and $P2X_3$ migrate as trimers when analyzed by blue native PAGE

As an alternative approach for the analysis of P2X oligomerization, we used blue native PAGE (Schägger

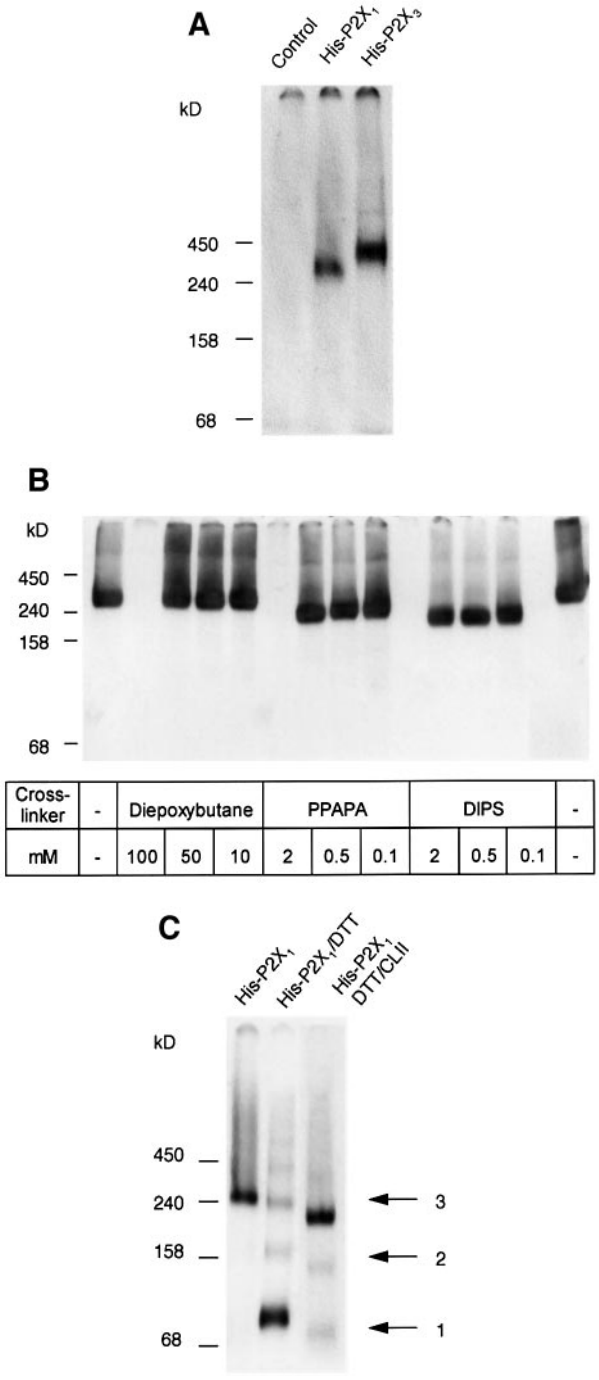

Fig. 4. Analysis of oligomerization of His-$P2X_1$ or His-$P2X_3$ subunits by blue native PAGE. Oocytes injected with cRNA for His-$P2X_1$ or His-$P2X_3$ were labeled overnight with [^{35}S]methionine and chased for 5 h. Digitonin (0.5%) extracts were prepared and P2X receptors purified by Ni^{2+}-agarose chromatography. All samples were supplemented with blue native sample buffer and analyzed by blue native PAGE and autoradiography. Numbered arrows indicate positions of P2X monomers, dimers and trimers. Mass markers: Combithek II™ (Boehringer Mannheim). (**A**) His-$P2X_1$ and His-$P2X_3$ were analyzed immediately after native elution (4–10% acrylamide gradient gel). (**B**) Purified His-$P2X_1$ was incubated with the indicated cross-linkers while still bound to the Ni^{2+}-agarose beads, then eluted with non-denaturing sample buffer and analyzed as above (5–16% acrylamide gradient gel). Note that the negatively charged cross-linkers PPAPA and DIPS increase electrophoretic mobility of His-$P2X_1$ adducts, whereas the uncharged cross-linker diepoxybutane does not. (**C**) His-$P2X_1$ unaltered or cross-linked with 0.5 mM CL II was supplemented with 0.1 M DTT (final concentration) and incubated for 30 min at 37°C prior to blue native PAGE (5–13% acrylamide gradient gel). Left lane, native His-$P2X_1$ incubated without DTT migrates as a trimer. Central lane, DTT induces an almost complete dissociation of native His-$P2X_1$ into dimers and monomers. The additional bands correspond to higher order P2X multimers and presumably reflect the enhanced aggregation state of proteins upon reduction of the disulfide bonds (Johnston and Südhof, 1990). Right lane, cross-linking largely prevents DTT-induced dissociation of the His-$P2X_1$ complex.

and von Jagow, 1991). His-$P2X_1$ isolated under non-denaturing conditions from digitonin extracts of oocytes appeared as a single protein band at 250–290 kDa (Figure 4A) depending on the percentage of acrylamide used for the preparation of the gel. The large mass previously tempted us to speculate that His-$P2X_1$ may be a pentamer or hexamer (Burnstock and Wood, 1996). It must be noted, however, that the electrophoretic mobility during blue native PAGE is determined by the excess of negative charges conferred to the analyzed protein by bound Coomassie Blue G dye. Since His-$P2X_1$ is rather basic (calculated pI 8.3), we examined whether the charge shift by Coomassie is insufficient and whether the molecular mass of $P2X_1$ receptors is overestimated when compared with the migration of less basic mass markers. Indeed, an increased electrophoretic mobility was observed when additional negative charges were conferred to His-$P2X_1$ by covalent binding of negatively charged cross-linkers (Figure 4B). The mobility increase correlated well with the number of negative charges of the cross-linkers. PPAPA, which carries only two negative charges, caused the smallest increase in mobility, whereas DIPS with four negative charges caused the largest increase in mobility (Figure 4B) and reduced the apparent molecular mass from 290 to ~200 kDa corresponding to a His-$P2X_1$ trimer. The uncharged cross-linker diepoxybutane had no effect on electrophoretic mobility. We conclude from these results that Coomassie binding may not suffice to render the electrophoretic mobility of His-$P2X_1$ entirely independent of its intrinsic basic charges.

To determine the number of subunits of His-P2X receptors by an approach that is independent of Coomassie and detergent binding and intrinsic charges, we elaborated conditions that induce a partial dissociation of the His-$P2X_1$ or His-$P2X_3$ complex. Exposure of natively eluted His-$P2X_1$ to the strong reductant dithiothreitol (DTT) in the presence of sodium 6-amino-*n*-caproate (Figure 4C), but also to Triton X-100 or urea (data not shown) prior to blue native PAGE induced the appearance of two additional protein bands besides the non-denatured His-$P2X_1$ complex. These proteins of apparent masses similar to 80 and 170 kDa represent the His-$P2X_1$ monomer and dimer, respectively, indicating that the non-denatured 250 kDa protein band must be a His-$P2X_1$ trimer. As expected, chemical cross-linking of His-$P2X_1$ with CL II prevented the dissociation of the trimers into dimers and monomers (Figure 4C). Similar results entirely consistent with His-$P2X_1$ trimers were obtained when dodecyl-β-D-maltoside instead of digitonin was used as a detergent for His-$P2X_1$ isolation.

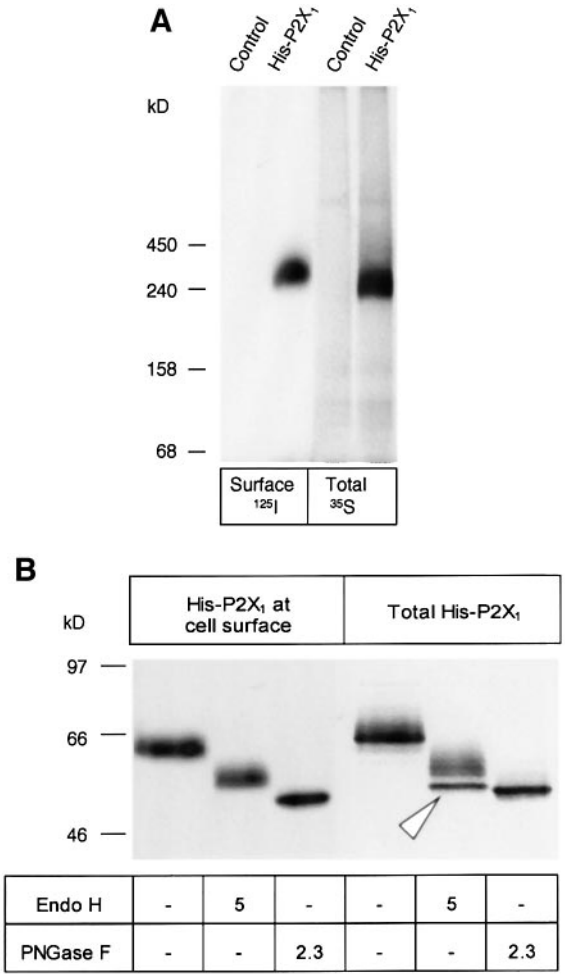

Fig. 5. Comparative analysis of surface-expressed His-$P2X_1$ and total His-$P2X_1$ (surface plus intracellular). (**A**) Oocytes injected with His-$P2X_1$ cRNA were kept for 3 days at 19°C and then labeled with membrane-impermeant ^{125}I-sulfo-SHPP. Subsets of the same oocytes were labeled with [^{35}S]methionine. His-$P2X_1$ was purified by Ni^{2+}-NTA chromatography from 1% digitonin extracts of each oocyte group, eluted with non-denaturing elution buffer, and resolved by blue native PAGE (4–10% acrylamide gradient gel) followed by autoradiography. (**B**) Aliquots of the same samples were supplemented with SDS sample buffer, 20 mM DTT, and Endo H or PNGase F as indicated (IUB milliunits). After 1 h of incubation at 37°C, proteins were resolved by SDS–PAGE (10% acrylamide) and visualized by autoradiography. The arrow indicates the fully Endo H-sensitive form of His-$P2X_1$ that is not observed at the plasma membrane.

Cell surface-expressed $P2X_1$ is a homo-trimer and carries Endo H-resistant and Endo H-sensitive N-glycans

Oocytes injected with His-$P2X_1$ cRNA and maintained for 2–3 days at 19°C express a large number of His-$P2X_1$ receptors in their plasma membrane, as evidenced by the large inward currents (–29 ± 3 μA, mean ± standard error, $n = 7$) that could be elicited in these cells by the first application of 1 μM ATP at holding potentials of –60 mV. However, detergent homogenates of [^{35}S]methionine-labeled oocytes include membrane proteins that are retained in the ER, en route to the plasma membrane or already in the plasma membrane. Since the retention of His-$P2X_1$ in the ER (Figure 1A) may reflect 'quality control' (Hammond and Helenius, 1995), the above results may be affected by incompletely folded, partially assembled or even misfolded His-$P2X_1$ receptors. To visualize the plasma membrane form of the His-$P2X_1$ receptor, we radio-iodinated oocyte surface proteins with ^{125}I-sulfosuccinimidyl-3-(4-hydroxyphenyl)proprionate (^{125}I-sulfo-SHPP), a lysine-reactive, membrane-impermeant compound. ^{125}I-labeled His-$P2X_1$ was then isolated by Ni^{2+}-NTA chromatography. When resolved by blue native PAGE, a single protein band was observed at 290 kDa corresponding in mass to total His-$P2X_1$ isolated from [^{35}S]methionine-labeled oocytes (Figure 5A). Partial dissociation with DTT in the presence of sodium 6-amino-*n*-caproate revealed that the ^{125}I-labeled His-$P2X_1$ complex

consisted of three His-$P2X_1$ monomers (results not shown) in agreement with data shown in Figure 4C.

Next, we compared the glycosylation status of surface His-$P2X_1$ with that of total His-$P2X_1$ (Figure 5B). Endo H diminished the mass of surface His-$P2X_1$ by 8 kDa (lane 2 from left), but was unable to release all the N-glycans. This indicates (i) that surface His-$P2X_1$ consists of an uniform protein population carrying both Endo H-sensitive and Endo-resistant N-glycans; and (ii) that at least one N-linked oligosaccharide side chain of all $P2X_1$ subunits of cell surface $P2X_1$ receptors must have been processed in the Golgi apparatus where complex-glycosylation occurs. In contrast, total His-$P2X_1$ consisted of at least two populations of proteins. One population could be completely deglycosylated with Endo H (indicated by an arrow in Figure 5B) and almost certainly represents His-$P2X_1$ not yet transported out of the ER. As expected, the ER form of His-$P2X_1$ was not observed at the plasma membrane (Figure 5B). The second population was only partially deglycosylated by Endo H and most likely corresponds to the surface form of His-$P2X_1$. Taken together, these data indicate that both the surface and the ER forms of His-$P2X_1$ consist of three His-$P2X_1$ monomers.

$P2X_1$ and $P2X_3$ receptors isolated with n-octylglucoside consist of trimers and hexamers

When 1% *n*-octylglucoside was used instead of digitonin or dodecyl-β-D-maltoside for receptor solubilization, blue native PAGE analysis revealed two protein bands that corresponded in size to the trimeric and hexameric form of His-$P2X_1$ and His-$P2X_3$ (Figure 6A). Omission of 6-amino-*n*-caproate from the standard sample buffer for blue native PAGE increased the yield of His-$P2X_1$ hexamers (Figure 6A). Tetramers or pentamers of His-$P2X_1$ were not seen. It must be noted, however, that the overall amount of His-$P2X_1$ that entered the gel was reduced in the absence of 6-amino-*n*-caproate. Hexamers were also observed when $P2X_1$ receptors were first solubilized in 1% octylglucoside and then washed and eluted from the beads in 1% digitonin and vice versa (data not shown). These findings indicate that hexamers were present whenever P2X receptors were exposed to octylglucoside. Once formed in octylglucoside, they were at least partially preserved in digitonin. Even larger aggregates of trimers such as nonamers, dodecamers and pentadecamers were produced when concentrated His-$P2X_1$ receptor samples were kept in octylglucoside (data not shown).

CHAPS and Triton X-100 were also examined as detergents for P2X receptor solubilization and found to produce less distinct protein bands when analyzed by blue native PAGE. We cannot rule out completely the possibility that a certain fraction of His-$P2X_1$ solubilized with CHAPS or Triton X-100 also migrated as a hexamer since a diffuse smear was consistently observed of approximately the mass of a hexamer in addition to His-$P2X_1$ trimers (data not shown).

To provide additional evidence for the occurrence of His-$P2X_1$ hexamers in *n*-octylglucoside, we performed cross-linking experiments. PPAPA produced dimers and trimers, whereas CL II produced a significant amount of hexamers besides the conspicuous trimers (Figure 6B). In addition, small amounts of tetramers and pentamers are

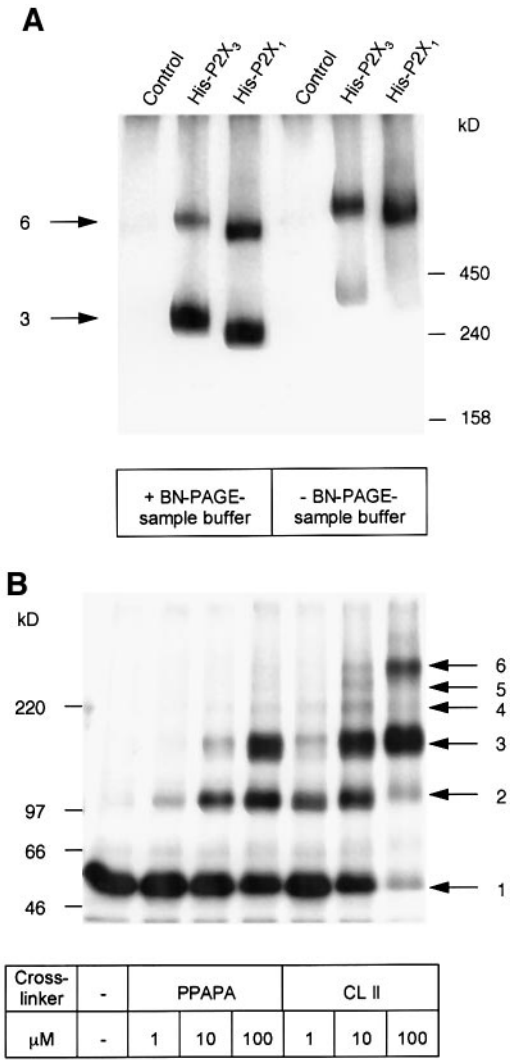

Fig. 6. Analysis of *n*-octylglucoside-solubilized His-$P2X_1$ and His-$P2X_3$ by blue native PAGE and cross-linking. Oocytes injected with cRNA for His-$P2X_1$ or His-$P2X_3$ were labeled overnight with [^{35}S]methionine. After a 5 h chase, *n*-octylglucoside extracts were prepared and P2X receptors were purified by Ni^{2+}-agarose chromatography. Samples were analyzed by blue native PAGE and autoradiography. (**A**) His-P2X receptors were isolated at 1% *n*-octylglucoside and supplemented (left panel) or not (right panel) with blue native (BN) sample buffer just before blue native PAGE (4–10% acrylamide gradient gel). (**B**) His-$P2X_1$ receptors isolated at 1% *n*-octylglucoside were cross-linked at the indicated concentrations of PPAPA and CL II. The samples were then supplemented with SDS sample buffer and resolved by non-reducing SDS–PAGE (4–10% acrylamide gradient gel) followed by autoradiography.

visible, particularly at 10 µM CL II. These results demonstrated that the hexameric complexes were not produced as an artifact of blue native PAGE analysis.

Blue native PAGE displays the correct pentameric architecture of the muscle-type nAChR synthesized in Xenopus oocytes

To further evaluate the present experimental approach, we expressed the muscle-type nAChR as a positive control in *Xenopus* oocytes. The pentameric architecture of nAChR with the subunit stoichiometry $(\alpha)_2(\beta 1)\gamma\delta$ is firmly established (Unwin, 1995; Hucho *et al.*, 1996). Two-electrode voltage clamp measurements on oocytes coinjected with

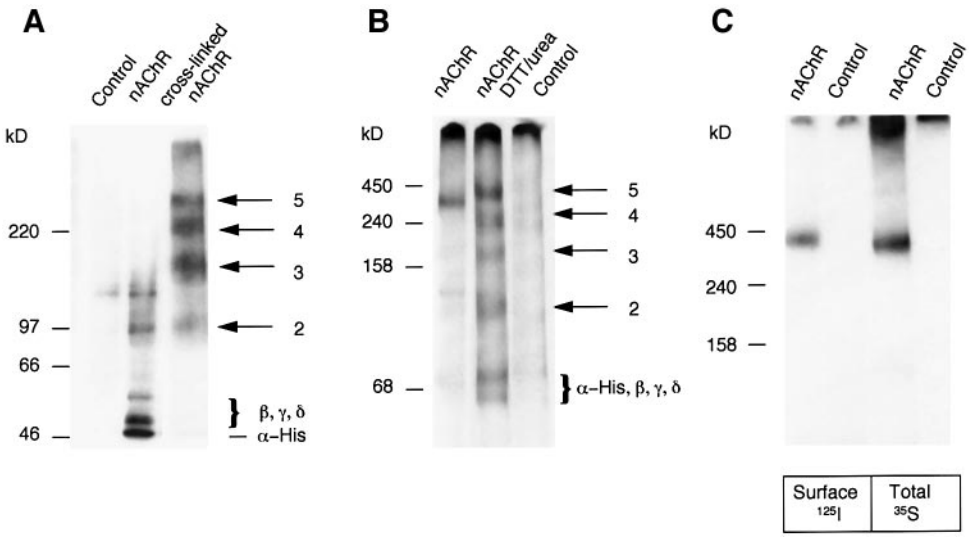

Fig. 7. Analysis of muscle-type nAChR by cross-linking and blue native PAGE. Oocytes were co-injected with cRNA (ratio 2:1:1:1) for the nAChR α_1-His_7 subunit and the non-tagged β_1, γ and δ subunits. After overnight labeling with [^{35}S]methionine and a 5 h chase interval or surface-labeling with ^{125}I-sulfo-SHPP, the nAChR was purified by Ni^{2+}-agarose chromatography from a dodecyl-β-D-maltoside (0.5%) extract. Numbered arrows indicate positions of dimer, trimer, tetramer and pentamer. (**A**) ^{35}S-labeled, purified nAChR was cross-linked at 5 mM DMS and resolved by reducing SDS–PAGE (4–10% acrylamide gradient gel) followed by autoradiography. Non-cross-linked nAChR was analyzed in parallel. (**B**) ^{35}S-labeled nAChR was supplemented with blue native sample buffer and analyzed by blue native PAGE (5–13% acrylamide gradient gel) and autoradiography. nAChR was analyzed as indicated without further treatment and after incubation with 0.1 M DTT and 8 M urea (added as a solid). Please note that rather harsh treatment was required to cause the heteromultimeric nAChR to dissociate into lower order intermediates. (**C**) Comparative analysis of surface-expressed and total nAChR (surface plus intracellular).^{125}I-sulfo-SHPP labeling of oocytes was performed 3 days after cRNA injection. ^{125}I-sulfo-SHPP-labeled and [^{35}S]methionine-labeled nAChR were resolved by blue native PAGE (4–10% acrylamide gradient gel) followed by autoradiography.

the cRNAs for β_1, γ, δ and either non-tagged α_1 or α_1-His_7 showed that the heptahistidyl sequence introduced at the C terminus of the α_1 subunit had no notable effect on the functional properties of the nAChR (data not shown). The non-tagged β_1, γ and δ subunits of the dodecyl-β-D-maltoside-solubilized nAChR were co-purified by Ni^{2+}-NTA chromatography together with the heptahistidyl-tagged α_1 subunit from *Xenopus* oocytes injected with the respective cRNAs (Figure 7A). All four individual subunits could be resolved by linear SDS–PAGE (data not shown). Treating natively eluted nAChR with 3,3′-dimethyl suberimidate (DMA) (Watty *et al.*, 1997) before the addition of SDS produced cross-linked nAChR pentamers besides intermediate stages (dimers, trimers and tetramers; Figure 7A). Blue native PAGE analysis of nAChR isolated from both surface-radioiodinated or metabolically labeled oocytes revealed one predominant band representing the pentameric receptor complex (Figure 7C). Incubating nAChR with DTT alone was insufficient to display lower order intermediates of nAChR by blue native PAGE. However, when nAChR was treated with DTT in the presence of 8 M urea, partial dissociation of nAChR resulted in the appearance of tetramers, trimers, dimers down to the monomers (Figure 7B). We conclude from these results that blue native PAGE combined with partial dissociation of the native receptor complex is able to display correctly the quaternary structure of ligand-gated ion channels.

Discussion

The present study not only brings a novel quaternary structure to ligand-gated ion channels, but also shows for the first time details of the biosynthesis of P2X receptors including N-glycosylation, homomeric assembly in the ER, processing of N-glycans subsequent to ER exit, and plasma membrane appearance of mature, homotrimeric P2X receptors. The demonstration of the usage of four out of five consensus sequences for N-glycosylation of $P2X_1$ places a large portion of the polypeptide chain on the extracellular side of the plasma membrane, strongly supporting the predicted membrane topology of P2X receptors. Consistent results obtained by both chemical cross-linking and blue native PAGE analysis of two P2X isoforms, $P2X_1$ and $P2X_3$, provide strong evidence that P2X receptors possess a trimeric architecture as discussed below. The extracellular domain of $P2X_2$ has recently been purified from bacteria and shown to form stable tetramers when refolded *in vitro* (Kim *et al.*, 1997). These results differ from those obtained with *Xenopus* oocytes, since truncated $P2X_3$ receptors that lack M2 are hindered from assembling into homomultimers in these cells (unpublished results). In a study performed before P2X receptors were cloned, a sedimentation coefficient of 12.1 S was found for a [^{3}H]α,β-methylene ATP-labeled protein thought to represent native P2X receptors (Bo *et al.*, 1992). Under identical conditions, we observed digitonin-solubilized His-$P2X_1$ trimers to sediment with the same high coefficient (data not shown).

Bifunctional antagonists as efficient cross-linkers of P2X receptors

Using structurally distinct cross-linkers with long spacers between two reactive groups, purified $P2X_1$ receptors could be quantitatively cross-linked to trimers of identical subunits. CL II, a derivative of the P2X receptor antagonist PPADS with a second reactive aldehyde group, turned out to be a particularly effective cross-linker and produced

covalently linked $P2X_1$ trimers at concentrations as low as 10 μM. To explain the high cross-linking efficiency of this compound, we assume that CL II, like PPADS itself, first becomes non-covalently bound to one binding site on the $P2X_1$ or $P2X_3$ receptor and then forms a Schiff base with a critical lysine residue. Once immobilized by one C=N bond, the second PPADS-like moiety of CL II may bind to the PPADS binding site on a neighboring $P2X_1$ subunit, an interaction that may be facilitated by the long and flexible spacer of CL II. A second C=N bond can then be formed between the free aldehyde group and a lysine residue of the neighboring $P2X_1$ chain. The view that interaction with the PPADS binding site favors cross-linking is supported by the finding that the ability of the three PPADS analogues to cross-link $P2X_1$ to homotrimers mirrored their order of potency as antagonists in functional experiments at $P2X_1$ receptors in rat vas deferens: CL II > DIPS > PPAPA (G.Lambrecht and B.Niebel, unpublished data). These results support the hypothesis that CL II and DIPS interact with $P2X_1$ ($P2X_3$) receptors according to the classical bivalent-ligand-mechanism (Portoghese, 1989).

Are full-sized P2X receptors trimers or hexamers?

Provided that either digitonin or dodecylmaltoside was used as a detergent for P2X receptor solubilization, chemical cross-linking never resulted in a complex larger than a trimer. Also when P2X receptors were solubilized in octylglucoside and then cross-linked with up to 100 μM PPAPA, no complexes larger than a trimer were produced. If, however, octylglucoside-solubilized $P2X_1$ receptors were cross-linked with CL II, covalently linked hexamers were observed in addition to trimers. Since only negligible amounts of intermediates such as tetramers and pentamers were produced, the hexamers were apparently formed by covalent pairing of two trimers, supporting the view that trimers constitute an essential structural element of P2X receptors.

Analysis of $P2X_1$ and $P2X_3$ receptor complexes by blue native PAGE yielded results that are consistent with the cross-linking experiments. The P2X receptors migrated quantitatively as trimers when purified in digitonin or dodecylmaltoside, whereas trimers and hexamers were observed when octylglucoside was used for receptor solubilization. Hexamers became the predominant or sole form of complex when purified P2X receptors were analyzed by blue native PAGE without prior addition of native sample buffer, suggesting that the native sample buffer impairs interactions between P2X trimers. Altogether, these results may be interpreted to show that octylglucoside is superior to digitonin or dodecylmaltoside as a detergent for P2X receptor solubilization and that P2X receptors are complexes of six identical subunits. However, for several reasons we argue that the formation of hexamers is artifactual. First, both digitonin and the frequently used dodecylmaltoside are mild detergents capable of preserving even weak protein–protein interactions (Schmalzing *et al.*, 1992, 1997). Secondly, aggregates composed of up to five $P2X_1$ trimers were observed when purified $P2X_1$ receptors were kept at a high receptor concentration in octylglucoside but not in digitonin. These findings suggest that octylglucoside favors aggregation upon random collisions of P2X trimers. Consumption of free sulfhydryls by iodoacetamide did not prevent the formation of these aggregates. Thirdly, hexamers were also observed when P2X receptors were first purified in octylglucoside and then kept in digitonin and vice versa, indicating that hexamer formation results from exposure to octylglucoside. Fourthly, the amount of $P2X_1$ multimers diminished when the concentration of octylglucoside was increased. At >1.5% octylglucoside, $P2X_1$ hexamers dissociated into smaller complexes down to monomers, implying that octylglucoside by itself possesses denaturing properties. Consistent with this possibility, P2X complexes stored in octylglucoside were much more sensitive to dissociating treatments such as heating, freezing and thawing, and incubation with DTT than when kept in digitonin. One striking difference between octylglucoside and dodecylmaltoside is the length of the hydrocarbon chain. Whereas the hydrocarbon chain of dodecylmaltoside has approximately the length of the fatty acyl chain of phospholipids, the hydrocarbon chain of octylglucoside is shorter and may be less able to shield hydrophobic surfaces through which P2X trimers are in contact with the lipid bilayer of natural membranes. Hence, hexamers or larger assemblies of trimers may be formed by hydrophobic interactions that can occur in octylglucoside but not in digitonin or dodecylmaltoside.

An attractive alternative possibility is that octylglucoside reveals a propensity of P2X trimers to combine to form larger complexes by exposing a subunit recognition site that also becomes exposed physiologically under particular conditions in living cells. Assuming that the trimeric P2X complex is the structural unit that mediates ATP-gated permeation of small cations, it is tempting to speculate that assembling two trimers into a hexamer may result in the formation of a much larger pore. Interestingly, the $P2X_7$ isoform exhibits a cation-selective conductivity that is typical for the whole P2X receptor family, but becomes slowly permeable to molecules as large as 1000 Da by an unknown mechanism when repeatedly stimulated with ATP, eventually leading to cytolysis (Surprenant *et al.*, 1996; Rassendren *et al.*, 1997b).

Trimerization of P2X monomers occurs in the ER

Assembly of most oligomeric membrane and secretory proteins occurs in the ER a few minutes after completion of synthesis and is a prerequisite for exit to the Golgi and later compartments (Green and Millar, 1995). In agreement with this general view, His-$P2X_1$ receptors purified after a 3 h [^{35}S]methionine pulse, while still largely within the ER, migrated entirely as trimers (data not shown). This suggests that trimerization took place in the ER soon after synthesis. Although P2X monomers must exist transiently in the ER, they remained undetected in the present experiments. In addition to the pool of $P2X_1$ trimers which is rapidly transported along the secretory pathway, we observed a significant fraction of $P2X_1$ trimers which remained resident in the ER. A similar behavior of influenza hemagglutinin, which also assembles to trimers that are partially retained in the ER, has been attributed to improper overall conformation of the transport-incompetent trimers (Copeland *et al.*, 1986). Likewise, we infer that trimerization of $P2X_1$ monomers alone is not sufficient to allow transport out of the ER and that incompletely folded P2X trimers are retained by

a phenomenon called 'quality control' (Hammond and Helenius, 1995).

Role of disulfide bonds

Dissociation of $P2X_1$ complexes into monomers was caused not only by DTT in the presence of sodium aminocaproate, but also by a variety of denaturing treatments which by themselves will not affect disulfide bonds, such as addition of urea or SDS. We conclude from these results that native P2X receptor complexes are maintained by non-covalent interactions and not by interchain disulfide linkages. It has to be mentioned, however, that low amounts of SDS-resistant $P2X_1$ oligomers up to hexamers which dissociated into monomers when treated with DTT were observed in the absence of reducing agents. Similar observations have been reported for influenza hemagglutinin (Boulay *et al.*, 1988) and synaptophysin (Johnston and Südhof, 1990). A detailed analysis has shown that disulfide cross-linking of synaptophysin occurs during solubilization by a disulfide exchange between closely adjacent cysteines in neighboring subunits (Johnston and Südhof, 1990). We could not, however, corroborate a reduction–oxidation cycle as a mechanism for $P2X_1$ polymerization during receptor purification since alkylation of free thiol groups by iodoacetamide did not prevent the occurrence of the SDS-resistant $P2X_1$ multimers. As an alternative possibility, disulfide cross-linked P2X subunits may be intermediates in normal protein folding, as has been suggested for thyroglobulin (Kim *et al.*, 1993), or misfolded ER forms. Consistent with this view, the amount of disulfide-linked $P2X_1$ subunits decreased during prolonged chase periods (data not shown).

The disintegration of P2X receptors caused by DTT requires additional comment. The presumed extracellular domain of a single P2X receptor subunit comprises 10 cysteine residues which are conserved among all family members (North, 1996b) and which may give rise to five intrachain disulfide linkages (Hansen *et al.*, 1997). Disulfide bonds are thought to have an important role in maintaining the mature conformation of proteins. This seems also to be true for P2X receptors, since blocking of disulfide formation on nascent $P2X_1$ subunits with DTT prevented $P2X_1$ trimerization and exit from the ER (unpublished results). Therefore, it was not unexpected to observe that $P2X_1$ complexes dissociated into monomers when the structural constraints imposed by disulfide bonds were removed by reduction with DTT. On the other hand, it is also known that the disulfide bonds of mature proteins are inaccessible to reducing agents unless denatured (Tatu *et al.*, 1993) and that functional P2X channels are remarkably resistant to chemical reduction with DTT (Rassendren *et al.*, 1997a). One may conclude from the DTT sensitivity of detergent-solubilized P2X receptors that they became partially denatured during purification. However, as mentioned above, the native sample buffer by itself possesses slight dissociating properties, most likely as a result of its sodium aminocaproate content. In the absence of native sample buffer, DTT treatment of detergent-solubilized $P2X_1$ caused little if any dissociation of $P2X_1$ trimers indicating that disulfide bonds were essentially as inaccessible to DTT as the disulfide bonds of P2X receptors of intact cells.

Pore-forming motifs and quaternary structure

Bundles of 4–6 approximately parallel transmembrane α helices are thought to represent a fundamental pore-forming motif of multiple channel proteins (Montal, 1996). The helices are arranged such that polar residues line the central hydrophilic pore and apolar residues face the hydrophobic bilayer interior. If each structural unit contributes solely one α helix to the pore, the number of structural units and the pore diameter or cation permeability should be closely related. The most selective channels, such as voltage-gated channels for Na^+ or Ca^{2+}, possess narrow pores of ~4 Å diameter that are thought to be formed by tetrameric bundles of α helices, one donated from each of four internally homologous domains. The less selective ion pore of the nicotinic acetylcholine receptor, for which a wealth of data exists, has an effective diameter of 6.5 Å (Dwyer *et al.*, 1980) and is lined by a bundle of five M2 helices, one from each subunit (Unwin, 1995; Hucho *et al.*, 1996). Channels of the glutamate receptor family that possess either a tetrameric (Laube *et al.*, 1998; Mano and Teichberg, 1998) or pentameric subunit organization (Ferrer-Montiel and Montal, 1996) have effective pore diameters between 5.5 Å (Villarroel *et al.*, 1995) and 7.8 Å (Burnashev *et al.*, 1996). Like the ionotropic receptors for acetylcholine and glutamate, P2X receptors are non-selectively permeable to cations including Ca^{2+} and possess an effective pore diameter slightly larger than that of the nAChR (Evans *et al.*, 1996). Given that the pore motif of P2X receptors consists also of a bundle of α helices contributed by M2, the proposed pore-forming segment (Rassendren *et al.*, 1997a), a tetrameric or pentameric subunit organization would be most plausible. A trimeric arrangement as suggested by the present study is not consistent with this pore motif, since a trimeric bundle of α helices can be expected to form an occluded pore. Also a hexameric subunit arrangement is not likely, since channels thought to be formed by a hexameric bundle of α helices such as members of the synaptophysin/connexin channel superfamily (Thomas *et al.*, 1988; Yeager and Nicholson, 1996) have pores as wide as 20 Å, allowing the passage of molecules up to ~1000 Da. These considerations may suggest that either our biochemical data are not consistent with the genuine quaternary structure or that P2X receptors must possess a pore motif distinct from the canonical bundle of α helices. There is evidence for the latter, since the inferred secondary structure of M2 of P2X receptors has evolved recently. Whereas initial structure predictions suggested the M2 segment to be α-helical, recent data obtained from extensive cysteine accessibility scanning imply that M2 of rat $P2X_2$ exists as a β strand (Rassendren *et al.*, 1997a). Unfortunately, with the exception of the helical-bundle motif and the porin β-barrel motif, there are virtually no pore structures of channel-forming membrane proteins at atomic resolution. Possible channel structures that emerge from crystallized soluble proteins and involve β barrels and mixed α/β folds have been discussed recently (Montal, 1996).

P2X receptors show no significant sequence homology to any characterized protein, but their membrane topology is reminiscent of a variety of other ion channels (for review see North, 1996a) such as the epithelial Na^+ channel/degenerin gene superfamily (Rossier *et al.*, 1994), the inwardly rectifying K^+ channels of eukaryotes and

bacteria (Schrempf *et al.*, 1995) and the mechanosensitive ion channel of *Escherichia coli* (Blount *et al.*, 1996). From these, inward rectifier K^+ channels are tetramers composed of identical or homologous subunits (Yang *et al.*, 1995). Epithelial Na^+ channels recently have been reported to have a tetrameric architecture as well, and to exist at the plasma membrane as heterotetramers of two α, one β and one γ subunit (Firsov *et al.*, 1998). However, there is also evidence for a heterononameric architecture of the same channels formed by three α, three β and three γ subunits (Snyder *et al.*, 1998). With respect to the pore structure there is evidence that epithelial Na^+ channels contain a hairpin structure similar to the lipophilic H5 segment of K^+ channels (Firsov *et al.*, 1998). P2X receptors also possess a highly conserved lipophilic domain immediately before M2, which was initially thought to be homologous to the H5 signature of K^+ channels and to contribute to the pore (Valera *et al.*, 1994). However, a H5 homologous sequence was only found in $P2X_1$ and not in the P2X isoforms identified later, and cysteine accessibility scanning provided no evidence that the residues in this region contribute directly to the aqueous pore (Rassendren *et al.*, 1997a). Hence, the oligomeric organization associated with pore formation of P2X receptors may be quite distinct from that of K^+ channels and epithelial Na^+ channels despite a similar overall membrane topology. A third channel protein with a P2X-like membrane topology, the mechanosensitive ion channel of *E.coli*, has been found by chemical cross-linking to consist of homohexamers (Blount *et al.*, 1996). Since this channel has a very large pore diameter of 34–46 Å (Cruickshank *et al.*, 1997), these data appear to support our view that a hexameric subunit arrangement is unlikely to account for the selectivity of P2X receptors for small cations. In a more general sense, our data together with those showing a hexameric architecture of the mechanosensitive ion channel of *E.coli* (Blount *et al.*, 1996) and a nonameric architecture of epithelial Na^+ channels (Snyder *et al.*, 1998) may be regarded as hints that some channels with a P2X-like membrane topology share a similar molecular architecture with trimers as the common denominator.

Blue native PAGE as a method for quaternary structure determination

As detailed above, chemical cross-linking and blue native PAGE analysis yielded results that were entirely consistent with each other. We could further substantiate the versatility of blue native PAGE by demonstrating that the muscle-type nAChR formed by co-expression of His-tagged α_1 subunit and the non-tagged β_1, γ and δ subunits migrated as a pentameric complex in agreement with the pentameric structure of this receptor (Unwin, 1995; Hucho *et al.*, 1996). Blue native PAGE should have broad applicability for the determination of the quaternary structure and subunit stoichiometry of ion channels, especially when combined with denaturing treatments that display individual channel subunits in addition to the multimeric complexes as shown here.

Altogether, our results indicate that P2X receptors possess a quaternary structure that is fundamentally distinct from the established tetrameric or pentameric subunit organization of the other families of ligand-gated ion channels. Further experiments are required to clarify unequivocally whether a trimer or a hexamer acts as the unit conduction element.

Materials and methods

cDNA constructs and transcripts

cDNAs comprising the complete coding sequences of $P2X_1$ (Valera *et al.*, 1994) and $P2X_3$ (Chen *et al.*, 1995; Lewis *et al.*, 1995) were amplified by RT–PCR from total RNA of rat vas deferens and rat adrenal gland, respectively, and cloned into vector pNKS2 (Gloor *et al.*, 1995). PCR primers used for RT–PCR were designed to introduce a unique *Nco*I site around the start codon of $P2X_1$ and $P2X_3$. Taking advantage of this site, codons for a hexahistidyl tag (His) could be inserted in-frame immediately before the start codon to yield His-$P2X_1$ and His-$P2X_3$. Mutant His-$P2X_1$-K249S (Lys249 is mutated to Ser) was generated using the Chameleon™ mutagenesis kit (Stratagene). Plasmids containing cDNAs for the α_1, β_1, γ and δ subunits of the rat muscle nAChR were kindly provided by Dr V.Witzemann (Witzemann *et al.*, 1990). A unique *Bam*HI recognition site was introduced at the stop codon of the α_1 subunit using the QuikChange™ mutagenesis kit (Stratagene). To generate nAChR α_1-His_7, double-stranded oligonucleotides encoding seven histidine residues followed by a stop codon were inserted in-frame between the engineered *Bam*HI site and a unique *Pvu*II site in the 3′ non-translated sequence of nAChR α_1 without changing any other amino acid. PCR-amplified P2X cDNAs, junction sequences and inserted oligodeoxynucleotides were sequenced by the dideoxynucleotide method.

Capped cRNAs were synthesized from linearized templates with SP6 RNA polymerase (Pharmacia), purified by Sepharose G50 chromatography and phenol–chloroform extraction, and dissolved in 5 mM Tris–HCl, pH 7.2, using the optical density reading at 260 nm for quantitation (OD_{260} 1.0 = 40 μg/μl).

Injection and maintenance of Xenopus oocytes

Xenopus laevis females were imported directly from South Africa. Follicle cell-free oocytes of oogenesis stages V or VI were obtained as described (Schmalzing *et al.*, 1992) and injected with 50 nl aliquots of cRNAs. Injected oocytes and non-injected controls of the same batch were cultured at 19°C in sterile ORi (oocyte Ringer's solution) (90 mM NaCl, 1 mM KCl, 1 mM $CaCl_2$, 1 mM $MgCl_2$ and 5 mM HEPES pH 7.4).

Metabolic labeling with [^{35}S]methionine and protein purification by Ni^{2+}-NTA chromatography

His-tagged P2X receptors were purified by Ni^{2+}-NTA agarose chromatography which has the advantage over immunoprecipitation that captured proteins can be eluted readily by competitive displacement with imidazole and/or by chelation of Ni^{2+} with no need for denaturing agents such as SDS. cRNA-injected oocytes and non-injected controls were metabolically labeled by overnight incubation with L-[^{35}S]methionine (>40 TBq/mmol, Hartmann Analytic, Braunschweig) at ~100 MBq/ml (0.4 MBq per oocyte) in ORi at 19°C and then chased for 5 h at 10 mM unlabeled methionine in ORi. Oocytes were homogenized in detergent buffer (20 μl/oocyte) consisting of 0.1 M sodium phosphate buffer pH 8.0, 1 mM phenylmethylsulfonyl fluoride, and the detergent indicated in the figures legends. Detergent extracts were cleared by centrifugation (10 min at 10 000 *g* and 4°C), diluted 5-fold with detergent buffer and supplemented with Ni^{2+}-NTA agarose (Qiagen) and imidazole–HCl pH 8.0 (final concentration 10 mM). After 30 min of end-over-end mixing at ambient temperature, beads were washed four times with ice-cold detergent buffer containing 25 mM imidazole–HCl pH 8.0. Protein was released from the Ni^{2+}-NTA agarose by two rounds of continuous gentle shaking, each for 10 min at ambient temperature, with non-denaturing elution buffer (pH 7.8) consisting of 20 mM Tris–HCl, 100 mM imidazole–HCl, 10 mM EDTA and the desired detergent. Eluted proteins were kept at 0°C until analyzed.

Cross-linking

1,2:3,4-diepoxybutane was from Aldrich, DIDS, DMS and DSP were from Sigma, and DTSSP was from Pierce. In search of more P2X-specific reagents, three distinct bifunctional analogues of the P2X receptor antagonist PPADS (Lambrecht *et al.*, 1992; Lambrecht, 1996) were synthesized. Details of the synthesis will be described elsewhere. In brief, PPAPA and DIPS were obtained by coupling diazotized 4-amino-benzaldehyde at pH 8.0 or diazotized 4,4′diaminostilbene-2,2′-disulfonic acid at pH 8.5, respectively, with pyridoxal phosphate. CL II was synthesized by reacting 4-nitrobenzoyl chloride with 2,2′-(ethylenedioxy)*bis*(ethylamine) in toluene at 80°C in the presence of Na_2CO_3. The resulting product was recrystallized, hydrogenated by catalytic reduction, diazotized, and then coupled with pyridoxal phosphate at pH 8.5. Finally, the cross-linkers were precipitated with isopropanol and found by silica gel thin-layer chromatography in isopropanol/33% NH_4OH/water (6:3:2) to be >96% pure. Structural formulae are shown in Figure 3.

Cross-linking was performed with purified His-P2X receptors before or after elution from the Ni^{2+}-NTA agarose as indicated in the figure legends. The reaction was initiated by adding a cross-linker from a freshly prepared stock solution in distilled water to purified protein in detergent buffer. DSP was added from a stock solution in DMSO. After 45 min at 37°C, at least 2 mol of $NaBH_4$ were added per 1 mol of PPADS-analogous cross-linker and incubation was continued for a further 15 min at 37°C. $NaBH_4$ reduces labile C=N double bonds to stable C–N single bonds. His-$P2X_1$ that was cross-linked while still bound to the Ni^{2+}-NTA agarose was washed with detergent buffer to terminate the cross-linking reaction and released from the beads with SDS sample buffer (final concentrations: 60 mM Tris–HCl, pH 6.8, 1% SDS, 10% glycerol, 0.1% bromophenol blue) or the non-denaturing elution buffer described above. Cross-linking of nAChR purified from cRNA-injected *Xenopus* oocytes was performed with 5 mM DMS in 0.2 M triethanolamine pH 8.5, for 1 h at ambient temperature (Watty *et al.*, 1997) after elution of dodecyl-β-D-maltoside-solubilized nAChR from the Ni^{2+}-NTA agarose.

Cell surface iodination

For selective labeling of P2X receptors at the plasma membrane, ^{125}I-sulfo-SHPP, a membrane-impermeant derivative of the Bolton-Hunter reagent was used (Thompson *et al.*, 1987). Three days after cRNA injection, oocytes were washed in oocyte-PBS (30 mM sodium phosphate, 70 mM NaCl, 1 mM $MgCl_2$, 0.1 mM $CaCl_2$) and placed in 0.5 ml tubes on ice. Sulfo-SHPP was iodinated at ambient temperature by rapid subsequent addition of 0.5 μg sulfo-SHPP (Pierce) in 2 μl of DMSO, 18.5 MBq of carrier-free $Na^{125}I$ (NEN), 10 μl of 5 mg/ml of chloramine T in 0.5 M sodium phosphate buffer pH 7.5, 100 μl of 1 mg/ml of DL-α-hydroxyphenylacetic acid in 0.1 M NaCl, and 10 μl of 12 mg/ml of sodium metabisulfite in 0.05 M sodium phosphate buffer pH 7.5. A 30 μl aliquot of this reaction mix was immediately added per 10–12 oocytes. After 60 min of incubation on ice with occasional gentle mixing, oocytes were rinsed with Ca-free ORi and extracted with the desired detergent in 0.1 M phosphate buffer pH 8.0. Proteins were purified by Ni^{2+}-NTA agarose chromatography as described above.

Blue native PAGE and SDS–PAGE

Blue native PAGE was carried out as described (Schägger and von Jagow, 1991; Schägger *et al.*, 1994) except that Serva blue G in cathode buffer A was used at 50 mg/l, and the stacking gel was omitted. Just before gel loading, purified proteins were supplemented with blue native sample buffer to final concentrations of 10% glycerol, 0.2% Serva blue G and 20 mM sodium 6-amino-*n*-caproate, and applied onto polyacrylamide gradient slab gels. Molecular mass markers (Combithek II™, Boehringer Mannheim) were run in two different lanes on both borders of the gel and were subsequently visualized by Coomassie staining. Gels were autoradiographed as described below.

For SDS–PAGE, protein samples were supplemented with SDS sample buffer either containing or lacking DTT, as indicated, and electrophoresed in parallel with [^{14}C]-labeled molecular mass markers (Rainbow™, Amersham) on SDS–polyacrylamide gradient gels. When indicated, samples were treated prior to SDS–PAGE with either Endo H or PNGase F (New England Biolabs) in the presence of 1% octylglucoside to diminish inactivation of PNGase F. Gels were fixed, dried and exposed to BioMax MR or MS film (Kodak) as appropriate at –80°C. In some experiments, radioactive bands were quantified with an image analyzer (Phosphor Imager 445 SI, Molecular Dynamics).

Electrophysiology

Current responses to ATP were measured by using the two-electrode voltage clamp technique on oocytes injected with P2X cRNA 2–4 days earlier. The electrodes contained 3 M KCl and had resistances of 0.3–1 MΩ. The superfusion solution consisted of 90 mM NaCl, 1 mM KCl, 2 mM $MgCl_2$ and 5 mM HEPES–NaOH pH 7.4. Calcium salts were omitted to avoid activation of endogenous Ca^{2+}-dependent Cl^- channels. ATP (1 μM) was applied for 5 s at 1 min intervals. Between measurements at different holding potentials, control responses were elicited by 1 μM ATP for 5 s at –60 mV. Only recordings from oocytes with no significant change in control responses at –60 mV throughout the experiment were included for analysis. A fast and reproducible solution exchange was achieved by using a 10 μl experimental oocyte chamber combined with a fast solution flow (150 μl/s) fed through a glass capillary mounted close to the oocyte. Current signals were low pass filtered at 100 Hz and sampled at 200 Hz using the Turbo TEC-05 amplifier (NPI electronics, Germany). All measurements were performed at room temperature (20–22°C).

Acknowledgements

We thank Dr V.Witzemann, Max-Planck-Institut für Medizinische Forschung, Heidelberg, for the nicotinic acetylcholine receptor plasmids and G.Spatz-Kümbel, Department of Biochemistry, University of Frankfurt, for the synthesis of PPADS-analogous cross-linkers. We also thank Dr Christine Piggee, Northeastern University of Boston, for linguistic help. The work was supported by grants of the Deutsche Forschungsgemeinschaft (La 350/7-1, Schm 536/2-1, and Graduiertenkolleg: 'Arzneimittelentwicklung und -analytik', University of Frankfurt) and the Fonds der chemischen Industrie.

References

Abbracchio,M.P. and Burnstock,G. (1994) Purinoceptors: are there families of P2X and P2Y purinoceptors? *Pharmacol. Ther.*, **64**, 445–475.

Anand,R., Conroy,W.G., Schoepfer,R., Whiting,P. and Lindstrom,J. (1991) Neuronal nicotinic acetylcholine receptors expressed in *Xenopus* oocytes have a pentameric quaternary structure. *J. Biol. Chem.*, **266**, 11192–11198.

Betz,H. (1990) Ligand-gated ion channels in the brain: the amino acid receptor superfamily. *Neuron*, **5**, 383–392.

Blount,P., Sukharev,S.I., Moe,P.C., Schroeder,M.J., Guy,H.R. and Kung,C. (1996) Membrane topology and multimeric structure of a mechanosensitive channel protein of *Escherichia coli*. *EMBO J.*, **15**, 4798–4805.

Bo,X., Simon,J., Burnstock,G. and Barnard,E.A. (1992) Solubilization and molecular size determination of the P_{2X} purinoceptor from rat vas deferens. *J. Biol. Chem.*, **267**, 17581–17587.

Boess,F.G., Beroukhim,R. and Martin,I.L. (1995) Ultrastructure of the 5-hydroxytryptamine$_3$ receptor. *J. Neurochem.*, **64**, 1401–1405.

Boulay,F., Doms,R.W., Webster,R.G. and Helenius,A. (1988) Posttranslational oligomerization and cooperative acid activation of mixed influenza hemagglutinin trimers. *J. Cell Biol.*, **106**, 629–639.

Buell,G., Collo,G. and Rassendren,F. (1996a) P2X receptors: an emerging channel family. *Eur. J. Neurosci.*, **8**, 2221–2228.

Buell,G., Lewis,C., Collo,G., North,R.A. and Surprenant,A. (1996b) An antagonist-insensitive P-2X receptor expressed in epithelia and brain. *EMBO J.*, **15**, 55–62.

Bültmann,R., Pause,B., Wittenburg,H., Kurz,G. and Starke,K. (1996) P_2-purinoceptor antagonists. I. Blockade of P_2-purinoceptor subtypes and ecto-nucleotidases by small aromatic isothiocyanato-sulphonates. *Naunyn-Schmied. Arch. Pharmacol.*, **354**, 481–490.

Burnashev,N., Villarroel,A. and Sakmann,B. (1996) Dimensions and ion selectivity of recombinant AMPA and kainate receptor channels and their dependence on Q/R site residues. *J. Physiol.*, **496**, 165–173.

Burnstock,G. (1996) Development and perspectives of the purinoceptor concept. *J. Auton. Pharmacol.*, **16**, 295–302.

Burnstock,G. and Wood,J.N. (1996) Purinergic receptors: their role in nociception and primary afferent neurotransmission. *Curr. Opin. Neurobiol.*, **6**, 526–532.

Cake,M.H., DiSorbo,D.M. and Litwack,G. (1978) Effect of pyridoxal phosphate on the DNA binding site of activated hepatic glucocorticoid receptor. *J. Biol. Chem.*, **253**, 4886–4891.

Chen,C.C., Akopian,A.N., Sivilotti,L., Colquhoun,D., Burnstock,G. and Wood,J.N. (1995) A P2X purinoceptor expressed by a subset of sensory neurons. *Nature*, **377**, 428–431.

Copeland,C.S., Doms,R.W., Bolzau,E.M., Webster,R.G. and Helenius,A. (1986) Assembly of influenza hemagglutinin trimers and its role in intracellular transport. *J. Cell Biol.*, **103**, 1179–1191.

Cruickshank,C.C., Minchin,R.F., Le Dain,A.C. and Martinac,B. (1997) Estimation of the pore size of the large-conductance mechanosensitive ion channel of *Escherichia coli*. *Biophys. J.*, **73**, 1925–1931.

Dani,J.A. and Mayer,M.L. (1995) Structure and function of glutamate and nicotinic acetylcholine receptors. *Curr. Opin. Neurobiol.*, **5**, 310–317.

Doms,R.W. and Helenius,A. (1986) Quaternary structure of influenza virus hemagglutinin after acid treatment. *J. Virol.*, **60**, 833–839.

Dwyer,T.M., Adams,D.J. and Hille,B. (1980) The permeability of the endplate channel to organic cations in frog muscle. *J. Gen. Physiol.*, **75**, 469–492.

Evans,R.J., Lewis,C., Virginio,C., Lundstrom,K., Buell,G., Surprenant,A. and North,R.A. (1996) Ionic permeability of, and divalent cation effects on, two ATP- gated cation channels (P2X receptors) expressed in mammalian cells. *J. Physiol.* (*Lond.*), **497**, 413–422.

Ferrer-Montiel,A.V. and Montal,M. (1996) Pentameric subunit stoichiometry of a neuronal glutamate receptor. *Proc. Natl Acad. Sci. USA*, **93**, 2741–2744.

Firsov,D., Gautschi,I., Merillat,A.M., Rossier,B.C. and Schild,L. (1998) The heterotetrameric architecture of the epithelial sodium channel. *EMBO J.*, **17**, 344–352.

Garcia-Guzman,M., Soto,F., Gomez-Hernandez,J.M., Lund,P.E. and Stühmer,W. (1997) Characterization of recombinant human $P2X_4$ receptor reveals pharmacological differences to the rat homologue. *Mol. Pharmacol.*, **51**, 109–118.

Gloor,S., Pongs,O. and Schmalzing,G. (1995) A vector for the synthesis of cRNAs encoding Myc epitope-tagged proteins in *Xenopus laevis* oocytes. *Gene*, **160**, 213–217.

Green,W.N. and Millar,N.S. (1995) Ion-channel assembly. *Trends Neurosci.*, **18**, 280–287.

Hammond,C. and Helenius,A. (1995) Quality control in the secretory pathway. *Curr. Opin. Cell Biol.*, **7**, 523–529.

Hansen,M.A., Barden,J.A., Balcar,V.J., Keay,K.A. and Bennett,M.R. (1997) Structural motif and characteristics of the extracellular domain of P2X receptors. *Biochem. Biophys. Res. Commun.*, **236**, 670–675.

Hollmann,M. and Heinemann,S. (1994) Cloned glutamate receptors. *Annu. Rev. Neurosci.*, **17**, 31–108.

Hucho,F., Tsetlin,V.I. and Machold,J. (1996) The emerging three-dimensional structure of a receptor. The nicotinic acetylcholine receptor. *Eur. J. Biochem.*, **239**, 539–557.

Johnston,P.A. and Südhof,T.C. (1990) The multisubunit structure of synaptophysin. Relationship between disulfide bonding and homo-oligomerization. *J. Biol. Chem.*, **265**, 8869–8873.

Kim,M., Yoo,O.J. and Choe,S. (1997) Molecular assembly of the extracellular domain of $P2X_2$, an ATP-gated ion channel. *Biochem. Biophys. Res. Commun.*, **240**, 618–622.

Kim,P.S., Kim,K.R. and Arvan,P. (1993) Disulfide-linked aggregation of thyroglobulin normally occurs during nascent protein folding. *Am. J. Physiol.*, **265**, C704–C711.

Kuner,T., Wollmuth,L.P., Karlin,A., Seeburg,P.H. and Sakmann,B. (1996) Structure of the NMDA receptor channel M2 segment inferred from the accessibility of substituted cysteines. *Neuron*, **17**, 343–352.

Lambrecht,G. (1996) Design and pharmacology of selective P2-purinoceptor antagonists. *J. Auton. Pharmacol.*, **16**, 341–344.

Lambrecht,G., Friebe,T., Grimm,U., Windscheif,U., Bungardt,E., Hildebrandt,C., Bäumert,H.G., Spatz-Kümbel,G. and Mutschler,E. (1992) PPADS, a novel functionally selective antagonist of P2 purinoceptor-mediated responses. *Eur. J. Pharmacol.*, **217**, 217–219.

Langosch,D., Thomas,L. and Betz,H. (1988) Conserved quarternary structure of ligand-gated ion channels: the postsynaptic glycine receptor is a pentamer. *Proc. Natl Acad. Sci. USA*, **85**, 7394–7398.

Laube,B., Kuhse,J. and Betz,H. (1998) Evidence for a tetrameric structure of recombinant NMDA receptors. *J. Neurosci.*, **18**, 2954–2961.

Lewis,C., Neidhart,S., Holy,C., North,R.A., Buell,G. and Surprenant,A. (1995) Coexpression of $P2X_2$ and $P2X_3$ receptor subunits can account for ATP-gated currents in sensory neurons. *Nature*, **377**, 432–435.

Lingueglia,E., Champigny,G., Lazdunski,M. and Barbry,P. (1995) Cloning of the amiloride-sensitive FMRFamide peptide-gated sodium channel. *Nature*, **378**, 730–733.

Lutter,L.C., Ortanderl,F. and Fasold,H. (1974) The use of a new series of cleavable protein-crosslinkers on the *Escherichia coli* ribosome. *FEBS Lett.*, **15**, 288–292.

Mano,I. and Teichberg,V.I. (1998) A tetrameric subunit stoichiometry for a glutamate receptor-channel complex. *NeuroReport*, **9**, 327–331.

Montal,M. (1996) Protein folds in channel structure. *Curr. Opin. Struct. Biol.*, **6**, 499–510.

Nayeem,N., Green,T.P., Martin,I.L. and Barnard,E.A. (1994) Quaternary structure of the native $GABA_A$ receptor determined by electron microscopic image analysis. *J. Neurochem.*, **62**, 815–818.

North,R.A. (1996a) Families of ion channels with two hydrophobic segments. *Curr. Opin. Cell Biol.*, **8**, 474–483.

North,R.A. (1996b) P2X receptors: a third major class of ligand-gated ion channels. *Ciba Found. Symp.*, **198**, 91–105.

Ortells,M.O. and Lunt,G.G. (1995) Evolutionary history of the ligand-gated ion-channel superfamily of receptors. *Trends Neurosci.*, **18**, 121–127.

Portoghese,P.S. (1989) Bivalent ligands and the message-address concept in the design of selective opioid receptor antagonists. *Trends Pharmacol. Sci.*, **10**, 230–235.

Rassendren,F., Buell,G., Newbolt,A., North,R.A. and Surprenant,A. (1997a) Identification of amino acid residues contributing to the pore of a P2X receptor. *EMBO J.*, **16**, 3446–3454.

Rassendren,F., Buell,G.N., Virginio,C., Collo,G., North,R.A. and Surprenant,A. (1997b) The permeabilizing ATP receptor, $P2X_7$—Cloning and expression of a human cDNA. *J. Biol. Chem.*, **272**, 5482–5486.

Rossier,B.C., Canessa,C.M., Schild,L. and Horisberger,J.D. (1994) Epithelial sodium channels. *Curr. Opin. Nephrol. Hypertens.*, **3**, 487–496.

Schägger,H. and von Jagow,G. (1991) Blue native electrophoresis for isolation of membrane protein complexes in enzymatically active form. *Anal. Biochem.*, **199**, 223–231.

Schägger,H., Cramer,W.A. and von Jagow,G. (1994) Analysis of molecular masses and oligomeric states of protein complexes by blue native electrophoresis and isolation of membrane protein complexes by two-dimensional native electrophoresis. *Anal. Biochem.*, **217**, 220–230.

Schmalzing,G., Kröner,S. and Passow,H. (1989) Evidence for intracellular sodium pumps in permeabilized *Xenopus laevis* oocytes. *Biochem. J.*, **260**, 395–399.

Schmalzing,G., Kröner,S., Schachner,M. and Gloor,S. (1992) The adhesion molecule on glia (AMOG/β2) and α1 subunits assemble to functional sodium pumps in *Xenopus* oocytes. *J. Biol. Chem.*, **267**, 20212–20216.

Schmalzing,G., Ruhl,K. and Gloor,S.M. (1997) Isoform-specific interactions of Na,K-ATPase subunits are mediated via extracellular domains and carbohydrates. *Proc. Natl Acad. Sci. USA*, **94**, 1136–1141.

Schrempf,H., Schmidt,O., Kummerlen,R., Hinnah,S., Muller,D., Betzler,M., Steinkamp,T. and Wagner,R. (1995) A prokaryotic potassium ion channel with two predicted transmembrane segments from *Streptomyces lividans*. *EMBO J.*, **14**, 5170–5178.

Snyder,P.M., Cheng,C., Prince,L.S., Rogers,J.C. and Welsh,M.J. (1998) Electrophysiological and biochemical evidence that DEG/ENaC cation channels are composed of nine subunits. *J. Biol. Chem.*, **273**, 681–684.

Surprenant,A., Rassendren,F., Kawashima,E., North,R.A. and Buell,G. (1996) The cytolytic P_{2Z} receptor for extracellular ATP identified as a P_{2X} receptor ($P2X_7$). *Science*, **272**, 735–738.

Tatu,U., Braakman,I. and Helenius,A. (1993) Membrane glycoprotein folding, oligomerization and intracellular transport: effects of dithiothreitol in living cells. *EMBO J.*, **12**, 2151–2157.

Thomas,L., Hartung,K., Langosch,D., Rehm,H., Bamberg,E., Franke,W.W. and Betz,H. (1988) Identification of synaptophysin as a hexameric channel protein of the synaptic vesicle membrane. *Science*, **242**, 1050–1053.

Thompson,J.A., Lau,A.L. and Cunningham,D.D. (1987) Selective radiolabeling of cell surface proteins to a high specific activity. *Biochemistry*, **26**, 743–750.

Unwin,N. (1995) Acetylcholine receptor channel imaged in the open state. *Nature*, **373**, 37–43.

Valera,S., Hussy,N., Evans,R.J., Adami,N., North,R.A., Surprenant,A. and Buell,G. (1994) A new class of ligand-gated ion channel defined by P2X receptor for extracellular ATP. *Nature*, **371**, 516–519.

Valera,S., Talabot,F., Evans,R.J., Gos,A., Antonarakis,S.E., Morris,M.A. and Buell,G.N. (1995) Characterization and chromosomal localization of a human P2X receptor from the urinary bladder. *Recept. Channels*, **3**, 283–289.

Villarroel,A., Burnashev,N. and Sakmann,B. (1995) Dimensions of the narrow portion of a recombinant NMDA receptor channel. *Biophys. J.*, **68**, 866–875.

Watty,A., Methfessel,C. and Hucho,F. (1997) Fixation of allosteric states of the nicotinic acetylcholine receptor by chemical cross-linking. *Proc. Natl Acad. Sci. USA*, **94**, 8202–8207.

Witzemann,V., Stein,E., Barg,B., Konno,T., Koenen,M., Kues,W., Criado,M., Hofmann,M. and Sakmann,B. (1990) Primary structure and functional expression of the α-, β-, γ-, δ- and ε-subunits of the acetylcholine receptor from rat muscle. *Eur. J. Biochem.*, **194**, 437–448.

Yang,J., Jan,Y.N. and Jan,L.Y. (1995) Determination of the subunit stoichiometry of an inwardly rectifying potassium channel. *Neuron*, **15**, 1441–1447.

Yeager,M. and Nicholson,B.J. (1996) Structure of gap junction intercellular channels. *Curr. Opin. Struct. Biol.*, **6**, 183–192.

Received December 9, 1997; revised April 2, 1998; accepted April 3, 1998